Indo-1 Fluorescence Signals Elicited by Membrane Depolarization in Enzymatically Isolated Mouse Skeletal Muscle Fibers

Vincent Jacquemond
Laboratoire de Physiologie des Eléments Excitables, UMR CNRS 5578, Université Claude Bernard, Lyon 1, F69622 Villeurbanne, France

ABSTRACT Indo-1 fluorescence signals were measured from one extremity of enzymatically isolated skeletal muscle fibers of mice. An original and simple method was developed to allow the measurements to be made under voltage-clamp control: the major part of a single fiber was embedded in silicone grease, so that only a short portion of one end of the fiber, from which the fluorescence measurements were taken, was in contact with the external solution. Membrane potential was held and varied by using a patch-clamp amplifier in whole-cell configuration with a single microelectrode, the tip of which was inserted across the silicone grease within the insulated portion of the fiber. In response to 100-ms depolarizing command pulses to voltages more positive than −40 mV (from a holding potential of −80 mV), clear changes in fluorescence were qualitatively observed to feature a time course of rise and decay expected from a change in intracellular calcium concentration ($[Ca^{2+}]_i$) due to voltage-dependent sarcoplasmic reticulum (SR) calcium release. Although the peak $[Ca^{2+}]_i$ elicited by a 100-ms depolarization at 0 or +10 mV varied from fiber to fiber, it could clearly reach a value high enough to saturate indo-1. The overall results show that this method represents an efficient way of measuring depolarization-induced $[Ca^{2+}]_i$ changes in enzymatically dissociated skeletal muscle fibers.

INTRODUCTION

In adult skeletal muscle, changes in free calcium due to SR calcium release, induced by controlled membrane depolarizations, have been extensively studied, providing numerous insights into the depolarization-contraction coupling process (for reviews see Schneider, 1994; Melzer et al., 1995). Over the past 15 years, most of these studies have been performed on amphibian and more recently on rat (Delbono and Stefani, 1993; Garcia and Schneider, 1993; Delbono, 1995; Garcia and Schneider, 1995; Delbono and Meissner, 1996; Shirokova et al., 1996) and human fibers (Delbono et al., 1995) isolated by mechanical dissection and mounted in a double vaseline-gap device. However, mechanical isolation of single mammalian skeletal muscle fibers is complicated by the high density of connective tissue, which makes the dissection process, requiring a high level of skill, not readily available to any interested candidate. On the other hand, the enzymatic dissociation of a whole muscle has proved to be a very efficient procedure for obtaining numerous intact viable and excitable isolated fibers (Bekoff and Betz, 1977; Head, 1993; Carroll et al., 1995). The enzymatic treatment, however, makes these fibers hard to manipulate, because no tendon is left at the ends of the fibers, and so far, no data concerning the changes in free calcium in response to voltage-clamp depolarizations have been available from such isolated fibers. I present here results from indo-1 fluorescence measurements performed on a voltage-clamped short portion of enzymatically isolated muscle fibers of mice. Voltage clamping was achieved with a single microelectrode, using a patch-clamp amplifier in the whole-cell mode. Results show that using such a simple method intracellular free calcium changes sharing the properties of calcium transients obtained on voltage-clamped, mechanically dissected rat fibers (Delbono and Stefani, 1993; Garcia and Schneider, 1993) can be measured on these enzymatically isolated fibers.

Received for publication 5 December 1996 and in final form 22 April 1997.

Address reprint requests to Dr. Vincent Jacquemond, Laboratoire de Physiologie des Eléments Excitables, Université Claude Bernard, Lyon 1, Bât. 401 B, 43 boulevard du 11 novembre 1918, F 69622 Villeurbanne Cedex, France. Tel.: 33-4-72-43-10-32; Fax: 33-4-78-94-68-20; E-mail: jacquemo@physio.univ-lyon1.fr.

0006-3495/97/08/920/09 $2.00

MATERIALS AND METHODS

Isolation of skeletal muscle fibers

Experiments were performed on intact isolated fibers from the flexor digitorum brevis muscles of mice. Mice were killed by diethyloxydediethylether anesthesia followed by cervical dislocation. Muscles were removed and incubated at 37°C for 90 min in a Tyrode solution containing collagenase (2 mg · ml^{-1}, Sigma type 1). Muscles were then rinsed with collagenase-free Tyrode solution and stored in Tyrode solution at 4°C until used. Isolated fibers were obtained by gently triturating the enzyme-treated muscles through the cut disposable tip of a Pipetman. Experiments were performed at room temperature (20–22°C).

Preparation of the isolated fibers

The experimental strategy consisted of electrically insulating a major part of the isolated fibers with silicone grease, so that whole-cell voltage clamping could be achieved with the patch-clamp amplifier on a short silicone-free portion of the fiber extremity. The bottom of the experimental chamber consisted of a glass coverslip, which was covered with a thin layer of silicone (silicone grease 70428; Rhône-Poulenc, Saint Fons, France). Isolation of the fibers from the enzyme-treated muscles was then performed directly within the chamber which, during that step, was filled with culture medium containing 10% bovine fetal serum (MI199; Eurobio, France). At that point, the presence of culture medium was critical: we indeed observed that in the presence of regular Tyrode as a bathing solution, most if not all of the isolated fibers developed a strong contracture when they came into contact with the silicone grease, which led to

irreversible damage of the fibers. Although the reason for the difference observed with culture medium was unclear and was not extensively studied, its use was definitely of great help because it prevented fiber contracture and termination. Fibers were left sitting on the silicone grease in these conditions for ~10 min, and the bathing medium was then replaced by the standard tetraethylammonium-$MeSO_3$-containing external solution. A single fiber was then covered with more silicone, so that 50–100 μm of its extremity was left free; this was performed by applying pressure through a silicone-filled glass micropipette with a broken tip, using a Picospritzer II apparatus (General Valve Corp., Fairfield, NJ). Intracellular indo-1 loading was then performed, as previously described (Allard et al., 1996), through local pressure microinjection with a micropipette containing 0.5 mM indo-1 (pentapotassium salt; Molecular Probes, Eugene, OR) dissolved in a 140 mM potassium aspartate-containing solution. In the experiments described throughout this paper, the indo-1 microinjection was always carried with the pipette tip inserted through the silicone grease into the insulated part of the fiber. After microinjection, the pipette was removed and the fiber was then left for 20–30 min before starting the experiment, so that the dye could diffuse until being homogeneously distributed throughout the entire volume of the cell. The insulated part of the fibers was firmly held by the silicone grease coating, so that when subthreshold depolarizing pulses were given, only the silicone-free end portion of the fiber was seen to contract.

Electrophysiology

An RK-300 patch-clamp amplifier (Bio-Logic, Claix, France) was used in whole-cell configuration. Command voltage pulse generation and data acquisition were done with commercial software (Biopatch Acquire, Biologic) driving an A/D, D/A converter (Lab Master DMA board, Scientific Solutions, Solon, OH). Analog compensation was used to decrease the effective series resistance. In a first series of trials, a patch pipette filled with a solution containing (mM): 110 potassium-aspartate, 20 KCl, 2 $MgCl_2$, 2 Na_2-ATP, 2 creatine phosphate, 2 K-HEPES, pH 7.0, was used; the tip was sealed on the silicone-free portion of fiber. However, that procedure was rapidly abandoned, because any contractile response elicited by sufficiently large depolarizing pulses tended to break the seal and irreversibly damage the fiber (not shown). Instead we used a microelectrode filled with a solution containing 3 M K-acetate and 20 mM KCl (typical resistance 1–3 MΩ). The tip of the microelectrode was inserted through the silicone, within the insulated part of the fiber, usually less than ~150 μm from the silicone-free extremity. Fig. 1 *A* (*right*) shows typical changes in current recorded in response to a 20-mV hyperpolarizing command pulse with the microelectrode tip first in the extracellular solution (*top trace*) and then in the silicone (*middle trace*), and finally after inserting the tip in the insulated part of the fiber (*bottom trace*). In that last situation, the holding command potential was set to −80 mV. From the measured change in current, the resistance was 1.7 MΩ in the bath, and went up to ~100 MΩ with the tip in silicone grease, which gives a lower limit to the "seal" resistance when the fiber was subsequently impaled. When the microelectrode tip was inserted in the fiber, the typical capacitive transients were observed in response to the 20-mV hyperpolarizing pulse. In two experiments, the free end of the fiber was completely covered with silicone after inserting the microelectrode in the fiber; under these conditions, the total resistance that could be measured was in the gigaohm range, which is indicative of the value of the seal resistance. Fig. 1 *B* shows a plot of the measured capacitance versus the membrane surface of the silicone-free extremity of fiber from distinct experiments. The capacitance was determined by integration of the control current elicited by a 20-mV hyperpolarizing pulse from the −80-mV holding potential, and the surface area was estimated from the measured length and width of the silicone-free fiber end, assuming that portion to be a cylinder. The data points fall quite well on a straight line with a fitted slope of 4.46 $\mu F \cdot cm^{-2}$. That value is somewhat higher than the ratio of transverse tubular system surface area to fiber surface area, found to be 3.1 cm^2/cm^2 in mouse extensor digitorum longus muscle fibers (Luff and Atwood, 1971). However, the discrepancy could be explained by a systematic underestimation of the surface area,

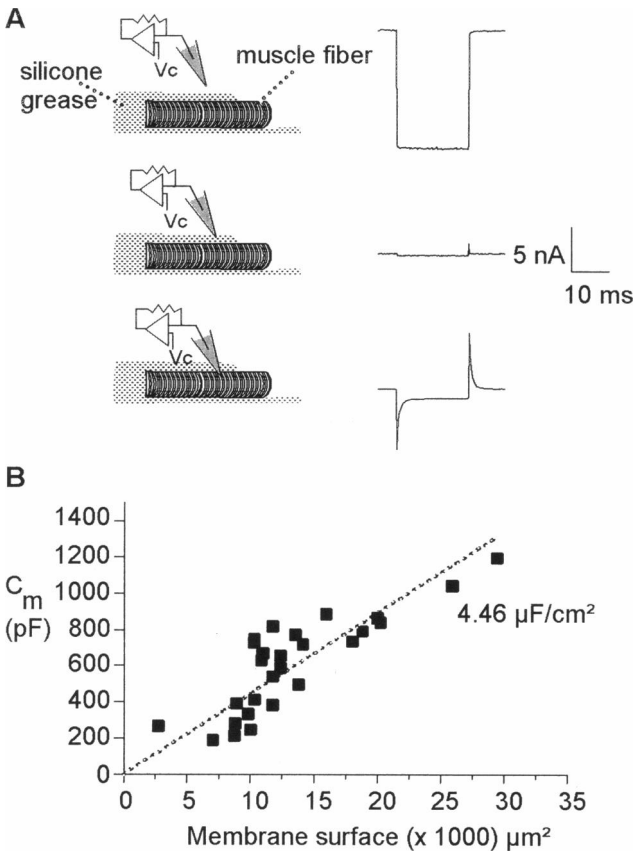

FIGURE 1 Voltage-clamping the free end of an isolated skeletal muscle fiber. (*A*) The cartoons on the left panel illustrate, from top to bottom, the successive steps of the procedure; the right panel shows the corresponding recorded changes in current in response to a −20-mV command voltage (V_c) step. The fiber is shown as a striated cylinder completely embedded in silicone grease (*grey area*), leaving the right extremity of the fiber free of silicone. The microelectrode and patch-clamp amplifier are schematized above the fiber. From top to bottom, the microelectrode tip is successively in the bath, then in the silicone coating, and finally within the fiber (across the silicone). Before the fiber was impaled with the microelectrode tip, the holding command potential was set at −80 mV. (*B*) Measured membrane capacitance as a function of the estimated surface membrane area of the silicone-free extremity of fibers. The capacitance was measured by integrating the current transient obtained in response to a −20-mV voltage step. The solid curve represents the result from fitting a straight line to the data points.

considering that, at the end of the fibers, the surface membrane has been shown to be strongly invaginated (Ishikawa et al., 1983). The mean surface area and the mean capacitance of the fiber segments used for the calcium measurements described in this paper were 12.3 ± 1 μm^2 and 540 ± 60 pF (n = 15), respectively.

All experiments were carried out at a holding command potential of −80 mV.

Fluorescence measurements

The optical set-up for indo-1 fluorescence measurements has been described elsewhere (Allard et al., 1996). In brief, a Nikon Diaphot epifluorescence microscope was modified to be used in diafluorescence mode. The beam of light from a high-pressure mercury bulb set on the top of the microscope was passed through a 335-nm interference filter, providing the excitation light for indo-1, and focused on the preparation using a quartz

aspherical doublet. The emitted fluorescence light was collected by a 40× objective and, through the use of a dichroic mirror and a set of appropriate optical filters, was simultaneously detected at 405 (F_{405}) and 470 nm (F_{470}) with a 10-nm bandwidth by two photomultipliers. Fluorescence signals were digitized and stored on disk, using the same hardware and software as for the electrophysiological measurements. The fluorescence measurement field was 40 μm in diameter, and the silicone-free extremity of each tested fiber was placed in the middle of the field. Indo-1 microinjected fibers were only UV illuminated during measurements, to minimize photobleaching. Background fluorescence at both emission wavelengths was measured on each tested fiber before indo-1 microinjection and then substracted from all measurements.

In vitro and in vivo calibration of the indo-1 fluorescence

Free calcium concentration ([Ca^{2+}]) was calculated using the now standard ratio method (Grynkiewicz et al., 1985), with the parameters $R = F_{405}/F_{470}$, R_{min} and R_{max} (the values of R in absence of calcium and in presence of an indo-1 saturating calcium concentration, respectively), K_D (the apparent dissociation constant for calcium binding to indo-1), and β (the ratio of F_{470} in the absence of calcium to F_{470} in the presence of a saturating calcium concentration). Early data from in vitro and in vivo indo-1 calibrations performed on the set-up were briefly reported previously (Allard et al., 1996), and the overall results are detailed here. Calibration solutions were prepared from two stock solutions containing (in mM) 100 KCl, 10 EGTA, 10 PIPES (piperazine-*N,N'*-bis-[2-ethanesulfonic acid]), pH 7.00, with and without 10 $CaCl_2$. Various free calcium concentrations were achieved by mixing these two stock solutions in different ratios. A high free calcium-containing solution was made by adding 1.5 mM $CaCl_2$ to the 10 mM $CaCl_2$-containing stock solution. Fig. 2 *A* illustrates the in vitro changes in F_{405} (*open squares*) and F_{470} (*open triangles*) versus [Ca^{2+}], measured from glass capillary tubes 50 μm in diameter, filled with the calibrating solutions to which 50 μM indo-1 was added. Data represent the mean (± SEM) of six different series of tube calibrations. As [Ca^{2+}] was increased, there was a clear rise in F_{405} and a slight decrease in F_{470}. Fitting the individual series of F_{405} data points by a 1:1 binding curve gave an apparent K_D value close to 0.35 μM (not shown). The open circles in Fig. 2 *B* correspond to the mean (± SEM) ratio values calculated from the individual series of fluorescence measurements. A 1:1 binding curve was fitted to the ratio data and is shown as a solid curve superimposed on the open circles in Fig. 2 *B*; the fit gave values of 0.44 μM, 0.27, and 1.78 for $K_D \cdot \beta$, R_{min}, and R_{max}, respectively.

The solid circles in Fig. 2 *B* show the values of R calculated from the fluorescence of cells equilibrated for 2 h in the presence of some of the calibration solutions also containing the ionophore 4-Br A23187 (20 μM) (Sigma), before being microinjected with indo-1; the R values are plotted versus the [Ca^{2+}] in the external solution. Results show that for the same [Ca^{2+}], the values of R appear to be larger in vivo than in vitro, which strongly suggests that the indo-1 fluorescence properties are modified by the cytoplasmic environment. Fitting the in vivo data points with a 1:1 binding curve gave a value of 0.65 μM for $K_D \cdot \beta$. Of course, the scattering in the data makes it hard to have full confidence in that value; however, considering that the β value was likely to be larger in vivo than in vitro (see below), it at least suggests that there was probably no strong shift in the apparent affinity of the dye in vivo as compared to in vitro. The in vivo values for R_{min} and R_{max} were checked regularly. For the series of experiments presented throughout this paper, R_{min} and R_{max} were assessed by using a procedure similar to the one described by Westerblad and Allen (1996): fibers were completely embedded in silicone, pressure microinjected with indo-1, and then, after dye equilibration, microinjected with a solution containing either 0.5 M EGTA or 1 M $CaCl_2$. This gave values for R_{min} and R_{max} equal to 0.53 ± 0.02 (n = 3) and 2.46 ± 0.19 (n = 6), respectively. The in vivo value of β was assessed using the method described by Bakker et al. (1993) and adapted by Westerblad and Allen (1996): the slope m from plots of F_{470} versus F_{405} was calculated from fluorescence transients elicited by membrane depolarizations such as the ones shown in Fig. 3. The mean value of m was −0.66 ± 0.02 (n = 37, from 13 fibers). β could then be calculated as $(1 - m \cdot R_{max})/(1 - m \cdot R_{min})$, which gave a value of 1.94. This value was definitely larger than the β value observed in vitro (~1.20 from data shown in Fig. 2 *A*).

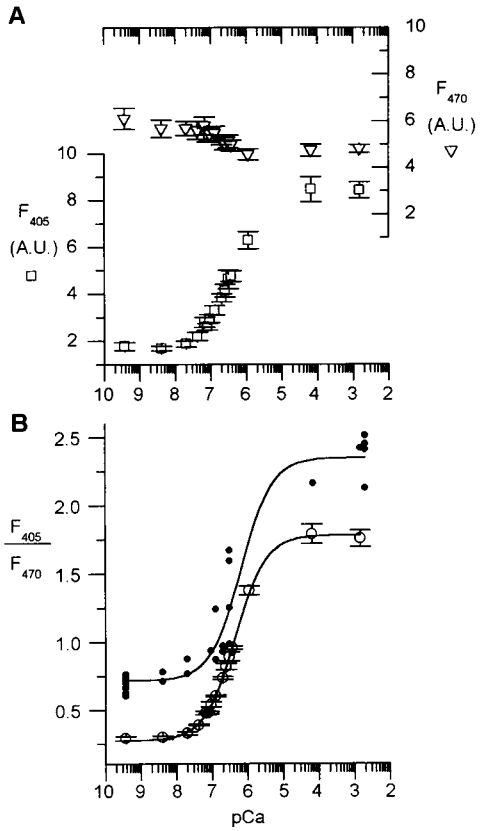

FIGURE 2 Calibration of indo-1 fluorescence. (*A*) In vitro fluorescence of indo-1 versus [Ca^{2+}]. Fluorescence at 405 (□) and 470 nm (△) in arbitrary units (A.U.) was measured from glass capillary tubes filled with [Ca^{2+}] calibration solutions containing 50 μM indo-1. Data correspond to the mean (± SEM) of six series of tube measurements. (*B*) Ratio of the indo-1 fluorescence at 405 and 470 nm versus [Ca^{2+}]. ○, Mean (± SEM) ratio values calculated from the individual fluorescence data, the mean of which is shown in *A*. ●, Points calculated from fluorescence measurements performed on fibers equilibrated for 2 h in the presence of the [Ca^{2+}] calibration solutions containing the ionophore 4-Br A23187 (20 μM), before being microinjected with indo-1.

Using the in vivo calibration parameters, the mean resting free calcium concentration at the start of the experiments was 21 ± 4 nM (n = 15).

Throughout this paper, the indo-1 ratio values were converted in terms of the indo-1 percentage of saturation, which corresponds to 100 times the fractional occupancy of the dye, calculated as $1/(1 + \{(R_{max} - R)/(\beta \cdot R - \beta \cdot R_{min})\})$.

Solutions and chemicals

The composition of the solutions used was (mM): Tyrode: 140 NaCl, 5 KCl, 2.5 $CaCl_2$, 1 $MgCl_2$, 10 HEPES, adjusted to pH 7.4 with NaOH; external solution: 140 TEA-methanesulfonate, 2.5 $CaCl_2$, 1 $MgCl_2$, 10 TEA-HEPES, and 0.001 tetrodotoxin, pH 7.4.

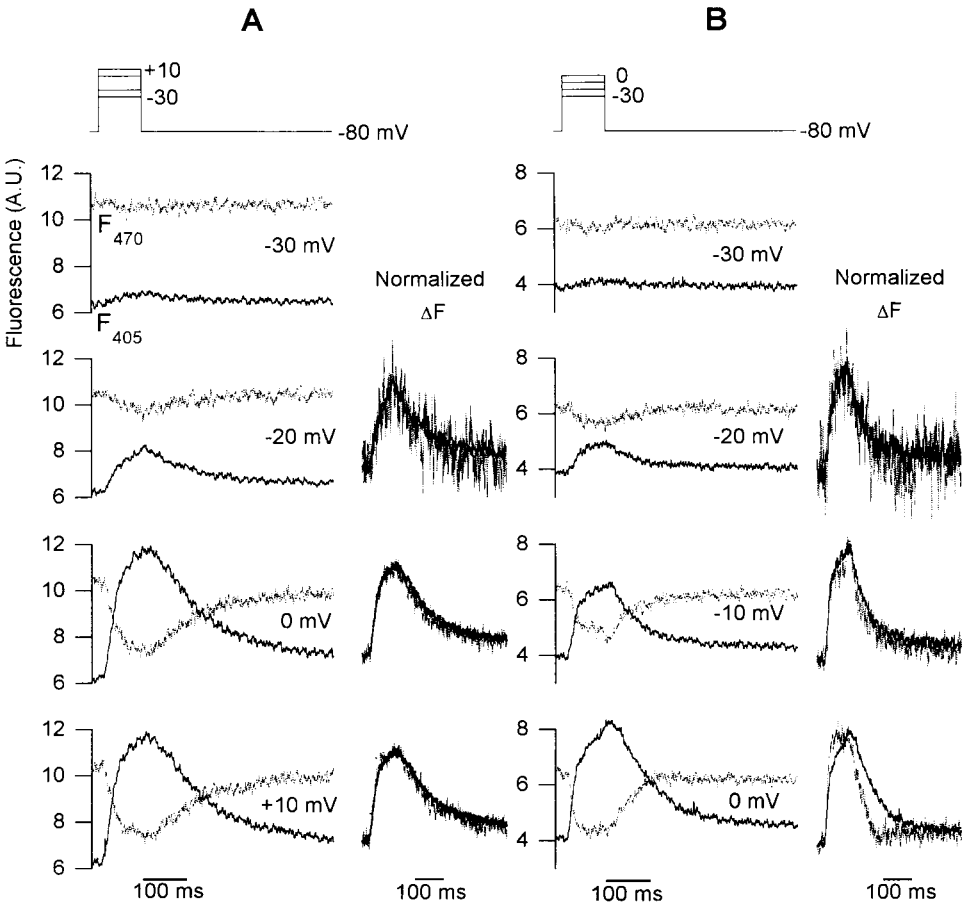

FIGURE 3 Fluorescence transients elicited by 100-ms command depolarizations of increasing amplitude in two different fibers (*A* and *B*). In *A* and *B*, the top traces show the pulse protocol. The series of traces shown below the pulse protocol correspond to the fluorescence records at 405 (upward-going traces, *solid line*) and 470 nm (downward going, *dotted line*) when changing the command voltage to the indicated value. The superimposed traces on the right panel correspond to the normalized changes in fluorescence (Normalized ΔF) at the two wavelengths for the depolarizations at, from top to bottom, −20, 0, and +10 mV (*A*) and −20, −10, and 0 mV (*B*), respectively. The ΔF_{470} traces (*dotted line*) were multiplied by −1 and then scaled up so as to display the same maximum amplitude as the corresponding ΔF_{405} (*solid line*).

Statistics

Least-squares fits were performed by using a Marquardt-Levenberg algorithm routine included in Microcal Origin (Microcal Software, Northampton, MA). Data values are presented as means ± SEM.

RESULTS

Fluorescence transients elicited by membrane depolarizations of various amplitudes

Fig. 3 shows fluorescence changes elicited by 100-ms depolarizing command pulses of various amplitudes from two distinct fibers (*A* and *B*). The pulse protocol is shown on the top of each series of fluorescence traces. The left panel of Fig. 3 *A* shows the simultaneously recorded fluorescence traces at 405 and 470 nm from a fiber depolarized by 100-ms command pulses to (from top to bottom) −30, −20, 0, and +10 mV, respectively. For the pulse to −30 mV, a small increase in F_{405} and a decrease in F_{470} could be measured, consistent with a detectable rise in myoplasmic Ca^{2+}. When applying a similar protocol in different fibers, detectable changes in fluorescence were first observed for a depolarization at −50, −40 mV, and −30 mV in one, three, and six fibers, respectively. In Fig. 3 *A*, the changes in fluorescence for the depolarizations at −20, 0, and +10 mV clearly consisted of a transient increase in F_{405} and a significant simultaneous transient decrease in F_{470}. If one were to consider the in vitro calibration of indo-1 (Fig. 2 *A*), an increase in calcium up to an indo-1 saturating level should not decrease F_{470} by more than 20% of its resting level. In Fig. 3 *A*, the transient change in F_{470} measured in response to the pulse to +10 mV decreased the fluorescence by 30% of its resting level, which again suggests that the fluorescence properties of indo-1 were altered in the cytoplasm as compared to in vitro, as already assessed from the results of the in vivo calibration (see Materials and Methods). The right panel of Fig. 3 *A* shows the changes in fluorescence (ΔF) measured at both wavelengths for the pulses to −20, 0, and +10 mV after scaling and normalization to the same maximum amplitude (Normalized ΔF): each ΔF_{470} trace was multiplied by a negative scaling factor, so that its peak matched the peak of the corresponding ΔF_{405} trace. The normalized ΔF_{405} (*solid curve*) and corresponding ΔF_{470} (*dotted curve*) traces are shown superimposed for each of the three depolarizations. It shows that the waveforms of the fluorescence transients at the two wavelengths were very similar, indicating that these transients are likely to be solely calcium-dependent and that there was no strong interference from movement artifacts. In Fig. 3 *B*, the fiber was depolarized with command pulses to −30, −20, −10, and 0 mV. The fluorescence transients qualitatively displayed a time

course similar to that in Fig. 3 *A*, with a clear voltage-dependent maximum change. After normalization (*right panel*), the waveforms of ΔF_{405} and ΔF_{470} were similar for the pulses to −20 and −10 mV, but quite different for the pulse to 0 mV, which suggests that, in that case, a movement artifact interfered with the calcium-dependent changes in fluorescence. Such movement artifacts were often detected in response to large depolarizing pulses, and should be canceled out by using the ratio F_{405}/F_{470} to calculate the corresponding $[Ca^{2+}]_i$ changes. It must be stressed, however, that, in a few cases, the depolarization-induced contraction had a deleterious effect on the fiber, provoking a strong irreversible rise in intracellular calcium and subsequent death of the fiber (not illustrated).

Ca^{2+} transients calculated from the indo-1 fluorescence signals

The time course and amplitude of the free calcium transient elicited by membrane depolarizations can be estimated from the change in ratio (F_{405}/F_{470}). The top panels of Fig. 4 show indo-1 percentage saturation traces calculated from ratios measured on two different fibers in response to 100-ms depolarizations of increasing amplitude (Fig. 4 *A*) and to depolarizations at −15 mV of increasing durations (Fig. 4 *B*), respectively. In Fig. 4 *A*, in response to the largest depolarizing pulse, indo-1 saturation reached a maximum of ~67%. In Fig. 4 *B* for the longest pulse, the maximum was ~60%. The bottom panels show the free calcium transients calculated from the above traces, assuming instantaneous equilibrium of the Ca-indo-1 reaction. In *A*, $[Ca^{2+}]_i$ increased during all pulses more positive than −40 mV; the initial rate of rise increased with the pulse amplitude, together with the size of the calcium transient, which reached a maximum close to 0.7 μM for the pulse to +20 mV. In *B*, the maximum amplitude of the calcium transient as well as its time to peak were increased with the pulse duration, whereas the time course of initial rise was very reproducible for the different pulses. For both sets of records, $[Ca^{2+}]_i$ slowly decayed back toward the resting

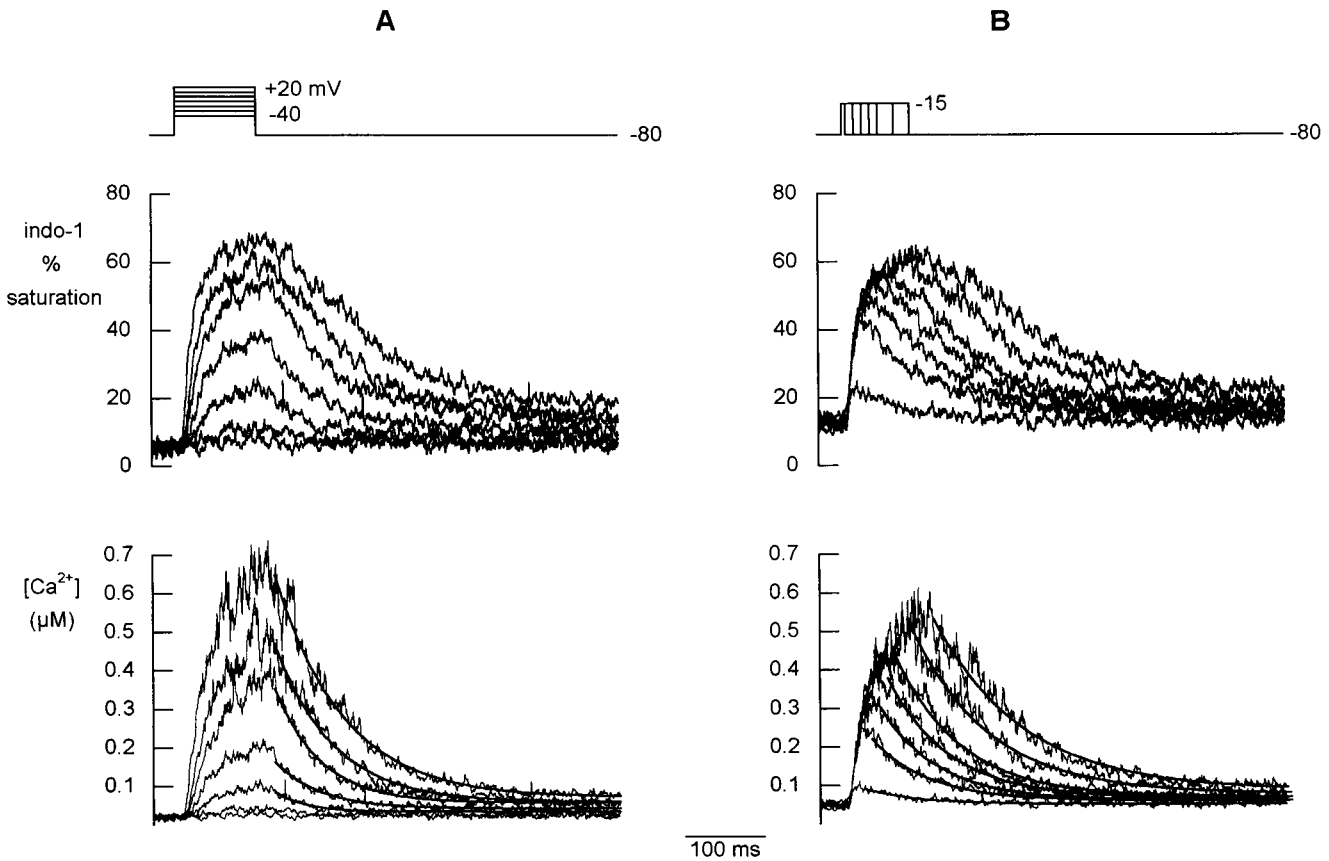

FIGURE 4 Changes in indo-1 percentage of saturation and corresponding calculated $[Ca^{2+}]$ transients elicited by depolarizing pulses of increasing amplitude or duration. Data shown in *A* and *B* were obtained from two different fibers. In *A* and *B*, the top traces show the pulse protocol, the middle series of traces correspond to the indo-1 percentage of saturation calculated from the ratio F_{405}/F_{470}, and the corresponding calculated $[Ca^{2+}]$ changes are shown on the bottom. In *A*, the fiber was stimulated by 100-ms command voltage pulses to −40, −30, −20, −10, 0, +10, and +20 mV. For the five largest depolarizations, the decay of the $[Ca^{2+}]$ traces was fitted with a single exponential plus constant function starting 20 ms after the end of the pulses. The fits are shown as solid curves superimposed on the decay of $[Ca^{2+}]$. (*B*) The fiber was stimulated by 5-, 15-, 25-, 35-, 45-, 65-, and 85-ms command pulses to −15 mV. The solid curves superimposed on the decay of the $[Ca^{2+}]$ traces correspond to the results from fitting a single exponential plus constant function.

level upon repolarization. The decay of the calcium transients was fitted with a single exponential plus constant function starting 20 ms after the end of the pulses. The fits are shown as solid curves superimposed on the decay of the Ca^{2+} transients. Fig. 5, *A* and *B*, shows plots of the fitted rate constants of decay and final steady levels, respectively, versus the peak $[Ca^{2+}]_i$ reached at the end of depolarizing pulses of various amplitudes or durations in different fibers. Data corresponding to results shown in Fig. 4 are shown as solid circles. Data shown in Fig. 5 were intentionally selected from six fibers from which a set of calcium transients elicited by depolarizations of various amplitude or duration were recorded, the maximum amplitude of which did not exceed 1 μM, this to avoid the complications introduced by strong dye saturation (see below). As the peak $[Ca^{2+}]_i$ was increased, there was a net tendency toward a decrease in the rate constant and a concomitant increase in the steady level, which are to be expected if a slowing of the calcium removal properties occurs as a result of increased occupancy of intrinsic calcium-binding sites (Melzer et al., 1986). Concerning the increase in $[Ca^{2+}]_i$ upon depolarization, although in some fibers it did seem to proceed along a single exponential time course, this was clearly not the case in all fibers or in the same fiber for different levels of depolarization, for which the $[Ca^{2+}]$ rising phases clearly presented a more complex waveform (data not shown).

Limitations introduced by indo-1 for accurately measuring Ca^{2+} transients

Measuring Ca^{2+} transients with a high-affinity dye such as indo-1 is highly likely to be limited by dye saturation when $[Ca^{2+}]$ exceeds the micromolar range. Fig. 6 shows a series of indo-1 percentage of saturation traces calculated from ratios obtained in response to successive 100-ms depolarizing command pulses of increasing amplitude. In this fiber, for pulses up to −20 mV, the peak of percentage of saturation and its initial rate of rise progressively increased with

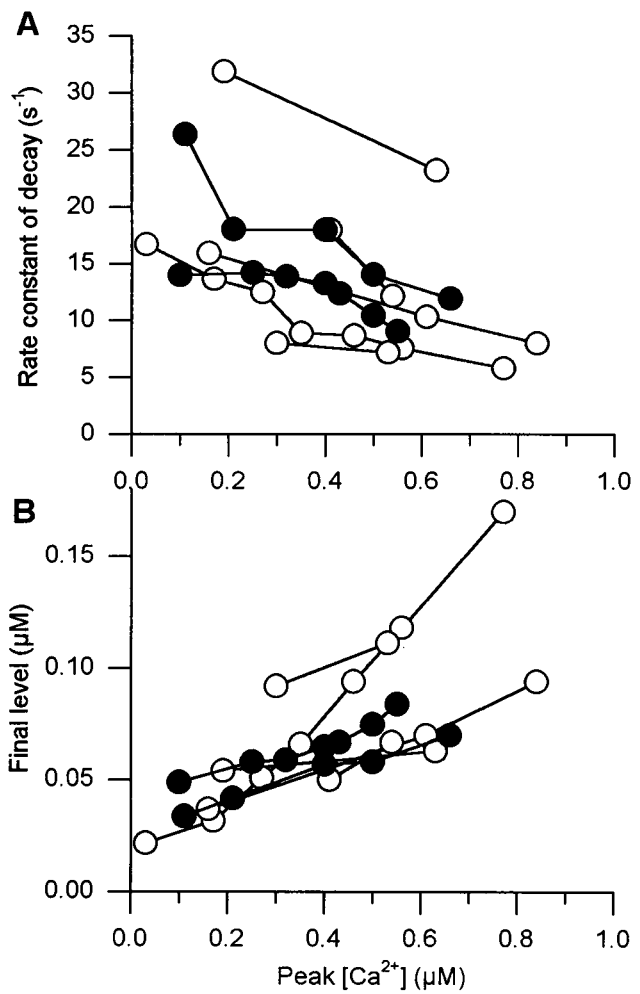

FIGURE 5 Effect of the peak $[Ca^{2+}]$ on the rate constant of $[Ca^{2+}]$ decay (*A*) and final $[Ca^{2+}]$ level (*B*) measured after the end of depolarizing pulses of various amplitudes or durations. The rate constants and final level values were obtained from fitting a single exponential plus constant function to the decay of $[Ca^{2+}]$ as shown in Fig. 4. Data from the two fibers shown in Fig. 4 are presented as filled symbols.

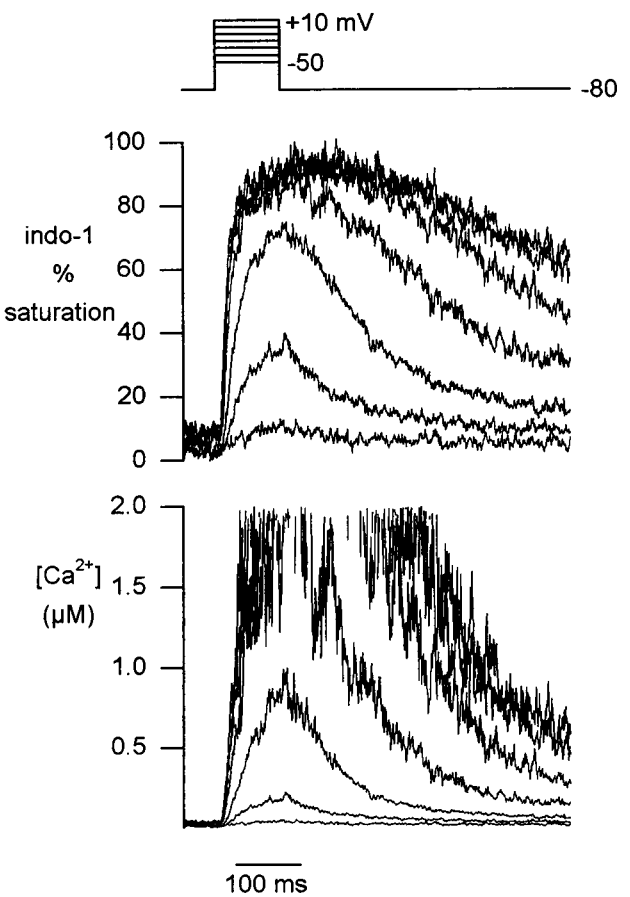

FIGURE 6 Indo-1 saturation in a fiber stimulated by 100-ms command voltage steps of increasing amplitude. The top panel shows the pulse protocol. The middle panel shows the indo-1 percentage of saturation traces calculated from the ratios F_{405}/F_{470}. The corresponding calculated $[Ca^{2+}]$ transients are presented in the bottom panel up to a maximum value of 2 μM.

the pulse amplitude. However, for the larger depolarizations, indo-1 rapidly approached full saturation, and the traces featured a sustained plateau-like phase followed by a very slow decay, which was distinguishable only late after the end of the pulses; under these conditions, considering the noise in the records, indo-1 saturation makes estimation of the time course and maximum amplitude of the free calcium transient highly uncertain. Fig. 6 *B* shows the corresponding free calcium transients displayed only with a *y* scale intentionally limited to a maximum of 2 μM; for the depolarizations above -20 mV, the free calcium transient definitely rose to a higher level, which was not accurately measurable with indo-1. These results also point out the variability of the maximum amplitude of the free calcium transient elicited by similar depolarizations from fiber to fiber. For instance, of 12 fibers from which indo-1 fluorescence was measured in response to a 100-ms pulse to -20 mV, the indo-1 saturation peaked at less than 80% in 10 fibers (mean corresponding peak $[Ca^{2+}]_i = 0.42 \pm 0.11$ μM) and at more than 80% in two fibers. In four fibers out of six, indo-1 saturation definitely peaked at more than 80% in response to a 100-ms pulse to 0 or +10 mV. The difficulty in measuring peak $[Ca^{2+}]$ values with indo-1 is further illustrated by the data shown in Fig. 7. Fig. 7, *A* and *B*, shows results from indo-1 fluorescence measurements performed on two distinct fibers, respectively. Both fibers were stimulated by five successive 100-ms command depolarizations to -20 mV. On the top row of Fig. 7 the five indo-1 percentages of saturation traces are shown superimposed. In Fig. 7 *A*, although the change in indo-1 saturation was not quite reproducible from one pulse to the next, it always reached a maximum between 40% and 50% in response to the successive voltage pulses. In Fig. 7 *B*, the maximum change in indo-1 saturation was more than 80% in response to all successive depolarizations. The second row of Fig. 7 shows the mean $[Ca^{2+}]$ (*solid line*) and SEM (*vertical dark bars*, *) calculated from the five corresponding indo-1 signals shown on the top row for each fiber, respectively. In Fig. 7 *A*, the maximum mean $[Ca^{2+}]$ was $\sim$0.3 μM, whereas in Fig. 7 *B* it reached a value more than 10 times larger. It should be noted that in Fig. 7 *B*, the rising phase of the $[Ca^{2+}]$ seemed to have a complex time course, with an initial fast increase followed by a secondary slower phase (indicated by an *arrow*), during which the $[Ca^{2+}]$ increased from $\sim$1 to more than 3 μM. That secondary rising phase could already be detected in the indo-1 percentage saturation traces, where it appeared as indo-1 saturation was $\sim$80% (also indicated by an *arrow*). However, as can be seen from the large increase in the corresponding standard error, the $[Ca^{2+}]$ was poorly determined during that secondary phase because of heavy indo-1 saturation. The graphs presented on the bottom row of Fig. 7 show the SEM versus the $[Ca^{2+}]$ for each of the two sets of measurements, respectively. The results definitely show that the measurement error dramatically increased as $[Ca^{2+}]$ rose in the upper micromolar range.

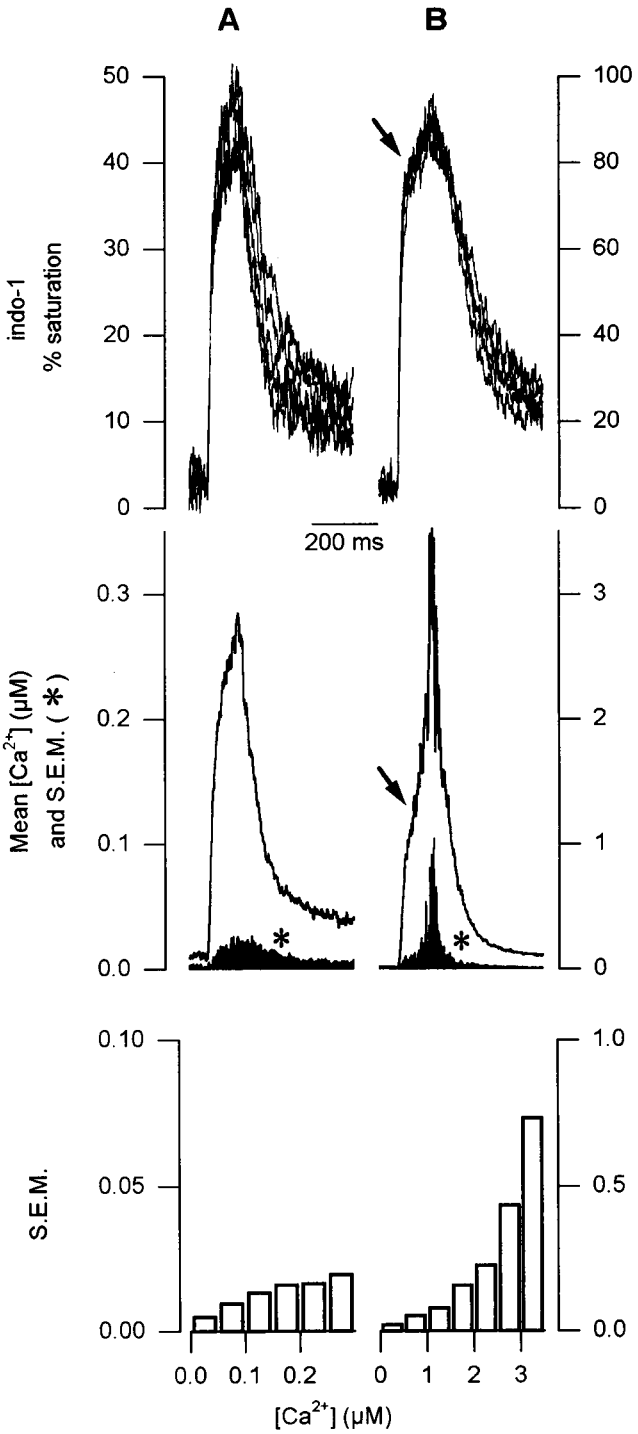

FIGURE 7 Indo-1 responses elicited by successive 100-ms depolarizing command pulses at -20 mV in two distinct fibers (*A* and *B*, respectively). The depolarizing pulses were delivered every 45 s. On the top row, the five consecutive indo-1 percentages of saturation traces are shown superimposed for each fiber. The second row shows the mean $[Ca^{2+}]$ (*solid line traces*) calculated for each fiber from the five indo-1 responses shown on the top row. The SEM is represented in the same plots by vertical dark lines (*). The graphs presented at the bottom show the SEM versus the $[Ca^{2+}]$ for each series of measurements. In *B*, the time course of rise of the percentage saturation traces presented a late slow component, which was responsible for a large increase above 1 μM of the corresponding mean $[Ca^{2+}]$ (both indicated by an *arrow*).

DISCUSSION

This paper shows that it is possible to elicit and control voltage-dependent calcium release in enzymatically isolated intact adult mouse skeletal muscle fibers. So far, in mouse skeletal muscle fibers, membrane depolarization-induced calcium transients have only been measured in response to action potentials or trains of action potentials (Turner et al., 1988; Westerblad and Allen, 1991, 1996; Carroll et al., 1995; Head, 1993). The results shown in the present paper reveal that, provided that the fibers were first left for some time, bathing in the presence of culture medium, they could be handled with an insulating greasy material, allowing voltage-clamp to be performed on a short portion of the fiber. The indo-1 fluorescence signals measured in response to step depolarizations proved the method to be efficient in eliciting and interrupting elevations in intracellular calcium, the maximum amplitude and rate of onset of which depend on the amplitude of the depolarization.

The calcium transients shown in this paper can be compared to the results obtained in rat cut fibers isolated by mechanical dissection, and mounted in a vaseline-gap device (Garcia and Schneider, 1993, 1995; Delbono, 1995; Delbono and Stefani, 1993). From Garcia and Schneider (1993), a change in intracellular calcium in response to 100-ms depolarizations of increasing amplitude could be detected at −40 mV with fura-2 in all tested fibers, and at about −20 mV with Antipyrylazo III, the difference being due to the higher affinity for calcium of fura-2. In the present experiments, the threshold for indo-1 to detect an increase in $[Ca^{2+}]_i$ was between −40 and −30 mV, and thus was similar to the value obtained with fura-2 in rat cut fibers, which is in agreement with these two dyes being more or less similar in terms of affinity for calcium (Grynkiewicz et al., 1985). In response to depolarizations of increasing amplitude, the onset of the $[Ca^{2+}]_i$ rise became faster and the peak $[Ca^{2+}]_i$ increased, as expected from a voltage-dependent increase in the rate of SR calcium release. Considering the maximum amplitude of the $[Ca^{2+}]_i$ transient in response to a depolarization of ~100 ms at 0 or +10 mV, Garcia and Schneider (1993) reported values between 0.15 and 2.2 μM, whereas Delbono and Stefani (1993) observed values in the 10 μM range. According to the present work, although it is hard to establish a comparable mean maximum value because of the variability observed from fiber to fiber and the uncertainty owing to indo-1 saturation, $[Ca^{2+}]_i$ was likely to peak in the several μM range in response to a 100-ms pulse to +10 mV. Considering the decline of the $[Ca^{2+}]_i$ transients upon repolarization, as long as $[Ca^{2+}]_i$ peaked at less than 1 μM, the decay could be reasonably fitted with a single exponential plus constant function. As the peak $[Ca^{2+}]_i$ was increased because of an increase in the amplitude or duration of the depolarizing pulse, the rate constant of decay was decreased and the final level was higher, which qualitatively agrees with previous observations on frog (Melzer et al., 1986) and rat (Garcia and Schneider, 1993; Delbono and Stefani, 1993) cut fibers, and indicates that the basic properties of the calcium removal systems are similar in enzymatically isolated intact mouse fibers under the present conditions. However, as compared to the rat cut fibers, the fitted rate of decay of the calcium transients appeared to be slower in our conditions. For instance, in response to depolarizing pulses of increasing durations, the rate constant of decay varied between 50 and 20 s^{-1} (Garcia and Schneider, 1993) and ~200 and 10 s^{-1} (from the time constants plotted in figure 8 of Delbono and Stefani, 1993). From the present data it was not possible to measure decay rates faster than ~30 s^{-1}. Although this could actually reflect either a lower overall rate of calcium removal from the myoplasm, or a prolonged continuation of SR calcium release after the end of the depolarizations, it is also possible that the limitations due to indo-1 binding kinetics and saturation make this dye unsuitable for accurately determining faster rates of $[Ca^{2+}]_i$ decay than reported here. A preliminary analysis of the effects of the response time of the dye (V. Jacquemond, unpublished observations) suggests that if the effective rate constants for the Ca^{2+}–indo-1 reaction in the myoplasm were reduced to an extent similar to that reported previously for fura-2 in skeletal muscle fibers (Baylor and Hollingworth, 1988; Garcia and Schneider, 1993) as compared to in vitro reports (Jackson et al., 1987; Lattanzio and Bartschat, 1991), this would not qualitatively change the observed dependence of the rate of $[Ca^{2+}]$ decay upon the peak $[Ca^{2+}]$. However, the typically observed maximum rate constants of decay of $[Ca^{2+}]$ reported here (15–20 s^{-1}) could then easily be underestimated by a factor of 2–10. Thus it is likely that the free calcium transients calculated here do not scrupulously reflect the true time course of change in free calcium and that future measurements using a lower-affinity, faster indicator should allow more accurate tracking of intracellular $[Ca^{2+}]$ transients (Zaho et al., 1996).

In conclusion, the method described here provides an easy, alternative way of studying some of the processes involved in the regulation of depolarization-induced $[Ca^{2+}]_i$ changes in intact skeletal muscle. Although the method cannot allow measurement of the mechanical work because the fiber is held by the silicone rather than mechanically, it should be useful for studies on isolated muscle fibers not easily accessible through manual dissection or on short muscle fibers that may be hard to mount in a vaseline-gap device.

I am strongly indebted to Dr. G. Christé for providing the idea of using culture medium to prevent fiber damage by the silicone grease, and to Dr. C. Ojeda for various enlightening suggestions while doing this work. I also thank Drs. B. Allard, J. C. Bernengo, C. Ojeda, O. Rougier, and Y. Tourneur for helpful suggestions and support.

This study was supported by the Centre National de la Recherche Scientifique (CNRS), the Université Claude Bernard, and a grant from the Région Rhône-Alpes.

REFERENCES

Allard, B., J. C. Bernengo, O. Rougier, and V. Jacquemond. 1996. Intracellular Ca^{2+} changes and Ca^{2+}-activated K^+ channel activation induced by acetylcholine at the endplate of mouse skeletal muscle fibres. *J. Physiol. (Lond.).* 494:337–349.

Bakker, A. J., S. I. Head, D. A. Williams, and D. G. Stephenson. 1993. Ca^{2+} levels in myotubes grown from the skeletal muscle of dystrophic (mdx) and normal mice. *J. Physiol. (Lond.).* 460:1–13.

Baylor, S. M., and S. Hollingworth. 1988. Fura-2 calcium transients in frog skeletal muscle fibres. *J. Physiol (Lond.).* 403:151–192.

Bekoff, A., and W. J. Betz. 1977. Physiological properties of dissociated muscle fibres obtained from innervated and denervated adult rat muscle. *J. Physiol. (Lond.).* 271:25–40.

Carroll, S. L., M. G. Klein, and M. F. Schneider. 1995. Calcium transients in intact rat skeletal muscle fibers in agarose gel. *Am. J. Physiol.* 269:C28–C34.

Delbono, O. 1995. Ca^{2+} modulation of sarcoplasmic reticulum Ca^{2+} release in rat skeletal muscle fibers. *J. Membr. Biol.* 146:91–99.

Delbono, O., and G. Meissner. 1996. Sarcoplasmic reticulum Ca^{2+} release in rat slow- and fast-twitch muscles. *J. Membr. Biol.* 151:123–130.

Delbono, O., K. S. O'Rourke, and W. H. Ettinger. 1995. Excitation-calcium release uncoupling in aged single human skeletal muscle fibers. *J. Membr. Biol.* 148:211–222.

Delbono, O., and E. Stefani. 1993. Calcium transients in single mammalian skeletal muscle fibers. *J. Physiol. (Lond.).* 463:689–707.

Garcia, J., and M. F. Schneider. 1993. Calcium transients and calcium release in rat fast-twitch skeletal muscle fibres. *J. Physiol (Lond.).* 463:709–728.

Garcia, J., and M. F. Schneider. 1995. Suppression of calcium release by calcium or procaine in voltage clamped rat skeletal muscle fibres. *J. Physiol. (Lond.).* 485:437–445.

Grynkiewicz, G., M. Poenie, and R. Y. Tsien. 1985. A new generation of Ca^{2+} indicators with greatly improved fluorescence properties. *J. Biol. Chem.* 260:3440–3450.

Head, S. I. 1993. Membrane potential, resting calcium and calcium transients in isolated muscle fibres from normal and dystrophic mice. *J. Physiol. (Lond.).* 469:11–19.

Ishikawa, H., H. Sawada, and E. Yamada. 1983. Surface and internal morphology of skeletal muscle. *In* Handbook of Physiology. Section 10: Skeletal Muscle. L. D. Peachey, R. H. Adrian, and S. R. Geiger, editors. American Physiological Society, Bethesda, MD. 1–21.

Jackson, A. P., M. P. Timmerman, C. R. Bagshaw, and C. C. Ashley. 1987. The kinetics of calcium binding to fura-2 and indo-1. *FEBS Lett.* 216:35–39.

Lattanzio, F. A., Jr., and D. K. Bartschat. 1991. The effect of pH on rate constants, ion selectivity and thermodynamic properties of fluorescent calcium and magnesium indicators. *Biochem. Biophys. Res. Commun.* 177:184–191.

Luff, A. R., and H. L. Atwood. 1971. Changes in the sarcoplasmic reticulum and transverse tubular system of fast and slow skeletal muscles of the mouse during postnatal development. *J. Cell. Biol.* 51: 369–383.

Melzer, W., A. Herrmann-Frank, and H. Ch. Lüttgau. 1995. The role of Ca^{2+} ions in excitation-contraction coupling of skeletal muscle fibres. *Biochim. Biophys. Acta.* 1241:59–116.

Melzer, W., E. Rios, and M. F. Schneider. 1986. The removal of myoplasmic free calcium following calcium release in frog skeletal muscle. *J. Physiol. (Lond.).* 372:261–292.

Schneider, M. F. 1994. Control of calcium release in functioning skeletal muscle fibers. *Annu. Rev. Physiol.* 56:463–484.

Shirokova, N., J. Garcia, G. Pizarro, and E. Rios. 1996. Ca^{2+} release from the sarcoplasmic reticulum compared in amphibian and mammalian skeletal muscle. *J. Gen. Physiol.* 107:1–18.

Turner, P. R., T. Westwood, C. M. Regen, and R. A. Steinhardt. 1988. Increased protein degradation results from elevated free calcium levels found in muscle from *mdx* mice. *Nature.* 335:735–738.

Westerblad, H., and D. G. Allen. 1991. Changes of myoplasmic calcium concentration during fatigue in single mouse muscle fibers. *J. Gen. Physiol.* 98:615–635.

Westerblad, H., and D. G. Allen. 1996. Intracellular calibration of the calcium indicator indo-1 in isolated fibers of *Xenopus* muscle. *Biophys. J.* 71:908–917.

Zaho, S., S. Hollingworth, and S. M. Baylor. 1996. Properties of tri- and tetracarboxylate Ca^{2+} indicators in frog skeletal muscle fibers. *Biophys. J.* 70:896–916.